Applied Catalysis B: Environment and Energy 354 (2024) 124135

Contents lists available at ScienceDirect

Applied Catalysis B: Environment and Energy

journal homepage: www.elsevier.com/locate/apcatb

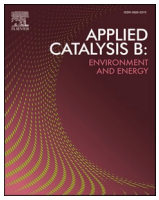

Regulating the synergy of sulfate and Pt species in Pt/ZSM-5 for propane complete oxidation

Lin-Ya Xu [a], Cai-Hao Wen [a], Xiao-Hui Luo [b], Wen-Xia Zhang [b], Xi Zhao [a], Qi-Hua Yang [a], Ji-Qing Lu [a], Meng-Fei Luo [a,*], Jian Chen [a,*]

[a] Key Laboratory of the Ministry of Education for Advanced Catalysis Materials, Zhejiang Key Laboratory for Reactive Chemistry on Solid Surfaces, Institute of Physical Chemistry, Zhejiang Normal University, Jinhua 321004, China
[b] Jinhua Polytechnic, Jinhua 321007, China

ARTICLE INFO

Keywords:
Propane complete oxidation
Pt supported catalyst
Sulfate modified
Pt/S atomic ratio
Synergetic catalysis

ABSTRACT

Modulating the active sites in atomic level is very meaningful to optimize catalyst performance but still very challenge. Herein, Pt catalysts loaded on different supports (ZSM-5, Al_2O_3, ZrO_2, CeO_2) were sulfate modified by in situ pyrolysis of $(NH_4)_2SO_4$ mixed with Pt catalyst. Sulfate remarkably improves these catalyst activities for propane combustion, particularly for the sulfate modified Pt/ZSM-5 catalyst with the highest activity among them. Through controlling the amount of $(NH_4)_2SO_4$ used and the loading of Pt, Pt/S atomic ratio in the sulfate modified Pt/ZSM-5 catalyst was successfully regulated. Pt/S atomic ratio significantly affects the electron transfer from Pt species to sulfate and also their interaction strength, which is decisive to the synergetic catalysis of sulfate and Pt species. The 5S-2Pt/ZSM-5 with Pt/S atomic ratio of 0.5 shows a moderate strength of sulfate and Pt species interaction, which is responsible for its highest reaction rate of 86.5 $\mu mol \cdot g_{Pt}^{-1} \cdot s^{-1}$ at 200 °C.

1. Introduction

Environmental pollution due to volatile organic compounds (VOCs) emission has drawn more and more attention recently, thus increasingly stringent environmental regulations are promulgated aimed at controlling VOCs emission [1–5]. Compared to adsorption, traditional thermal combustion, and emerging photo-catalysis, catalytic oxidation technology is widely employed in the field of VOCs elimination owing to its remarkable advantages of high efficiency, low operating temperature, and harmless products [6–9]. Among all the VOCs, light alkane with stable structure is mostly difficult to be oxidized, whereas light alkanes are massively produced from vehicles exhaust, petroleum industrial processes, and F-T synthesis exhaust gas [10–21]. Therefore, it is highly recommended to explore a efficient and low-temperature oxidation catalyst for the removal of light alkane exhaust gas. To the best of our knowledge, noble metals such as Pt and Pd based catalysts are generally regarded as the most active catalysts for light alkane oxidation compared to those transition metal based catalysts, Ru based catalyst has also been employed in propane combustion recently [22–24]. However, the scarcity and continuously rising prices of noble metal would severely hinder the massive application of noble metal catalysts, thus the development of more active noble metal based catalyst and increasing utilization efficiency of noble metal is in urgent need.

Recently, propane is frequently used as a model reactant to develop the active catalyst for VOCs abatement [25–28]. More efforts have been mainly paid into improving catalytic activity, and deeply understanding the surface active and reaction mechanism of platinum based catalyst for propane complete oxidation. Usually, the role of support and transition metal oxides promoter on Pt based catalyst has firstly gained most research attentions. Support commonly affects the chemical state of Pt species, thus changing the performance of catalyst for propane oxidation. Yazawa *et al.* studied the support effect on the low temperature propane complete oxidation over platinum catalyst loaded different supports (MgO, La_2O_3, ZrO_2, Al_2O_3, SiO_2, SiO_2-Al_2O_3, and SO_4^{2-}-ZrO_2), they claimed that acid strength of support materials affects the catalytic activity by controlling the platinum oxidation-resistance under the oxidizing atmosphere, because the electrophilic/electrophobic of property support materials is closely related to its acid strength [29,30]. Wang *et al.* also demonstrated that Pt/ZSM-5 with low Si/Al ratio exhibits superior catalytic activity for propane oxidation under dry reaction condition because the abundant acid sites favor the existence of highly dispersed Pt species and promote the propane activation [31].

* Corresponding authors.
E-mail addresses: mengfeiluo@zjun.cn (M.-F. Luo), jianchen@zjnu.cn (J. Chen).

https://doi.org/10.1016/j.apcatb.2024.124135
Received 7 January 2024; Received in revised form 22 April 2024; Accepted 26 April 2024
Available online 28 April 2024

CeO_2 support is widely used to load Pt catalyst for CO oxidation due to its excellent ability to store oxygen and disperse Pt species, however, Pt/CeO_2 catalyst usually shows inferior activity for propane oxidation in comparison with Pt/ZSM-5 catalyst, this result can be ascribed to its insufficient acid sites. With respect to the transition metal oxide promoter, most of the research has been focused on those acid or reducible oxides (WO_3, MoO_3, Nb_2O_5, V_2O_5, etc) to modify Pt catalysts employed propane oxidation [32–35]. The researchers generally recognize that these transition metal oxide promoters could enhance the propane oxidation activity of Pt catalyst by promoting oxidized Pt species reduction, increasing the acidity of support, our group also pointed out that the generation of active interface between noble metal and transition metal oxides leads to the accelerated catalytic reaction [36,37]. However, the limited kinds of transition metal oxides hinders the development of promoter modified Pt catalyst by this strategy.

Besides the metal oxide promoter, sulfate modified Pt catalysts are also extensively investigated for propane oxidation. It is very interesting to find that sulfate substances often induces the deactivation of Pt based catalyst such as for catalyzing CO or methane oxidation [38]. Whereas, sulfate modified Pt catalyst indeed exhibits superior catalytic activity for propane, ethyl acetate, ethanol oxidation such as sulfate modified Pt/TiO_2, Pt/ZrO_2, Pt/Al_2O_3, Pt/CeO_2 [39,40]. These results obviously indicates the different demand of active sites for propane oxidation in comparison with CO or methane oxidation. It is commonly recognized that the geometric structure and electric state of Pt active sites significantly affect the performance of Pt based catalyst for propane oxidation. Metallic state Pt species is usually believed to be active for alkane adsorption and C-H bond activation, and subsequently the intermediate products complete oxidation occur over oxidized Pt species [41]. Thus, the activation of C-H bond is commonly considered as the reaction initial and rate-determined step for propane oxidation. However, the activation of C-C bond in the propane by sulfate modified Pt catalyst is believed to significantly improve the activity. For instance, solid acid catalyst is active for C-C bond activation, thus usually employed to catalyze alkane isomerization reaction [42]. Sulfate modified ZrO_2 support, as the super solid acid, also shows superior catalytic activity for propane oxidation compared to the parent ZrO_2 support at high reaction temperature [43]. The synergetic catalysis of sulfate and Pt species may play crucial role on enhancing the catalytic activity of sulfate modified catalyst for propane oxidation. Whereas, it is still very difficult to correctly describe the interaction between sulfate and Pt species, and the mechanism of their synergetic catalysis. How to regulate the synergy of sulfate and Pt species in Pt catalyst for propane complete oxidation is still very challenge.

It is well known that traditional method for sulfate modified Pt catalyst often uses excessive sulfuric acid to treat oxides support (Al_2O_3, ZrO_2, CeO_2, etc) [29,30,43,56], which causes the serious environmental pollution and thus limits the practical application of those catalysts due to large waste sulfuric acid emission. Therefore, developing innovative method to modify Pt catalysts, without usage of sulfuric acid, is highly attractive for the development of practical catalysts. Herein, we prepared Pt catalysts loaded on different support (ZSM-5, Al_2O_3, ZrO_2, CeO_2), and these as-prepared Pt catalysts were facilely modified by sulfate species by in situ pyrolysis of only small amount of $(NH_4)_2SO_4$ mixed with Pt catalyst. Such novel strategy can effectively modify sulfate on Pt catalyst and avoid the usage of liquid sulfuric acid and emission of waste acid compared to the traditional sulfuric modification method [39,43]. Additionally, the Pt/S atomic ratio can be successfully regulated in the sulfate modified Pt catalyst by controlling the amount of $(NH_4)_2SO_4$ used and the loading of Pt. It is very challenge to evaluate the interaction strength of sulfate and Pt species, and the effect of such interaction strength on catalytic activity in sulfate modified Pt catalyst. Through the CO chemical uptake characterization, we propose an novel method to calculate the relative interaction strength of sulfate and Pt species which is affected by Pt/S atomic ratio. The synergetic catalysis of sulfate and Pt species affected by the their interaction strength is deeply revealed for propane oxidation. This work also provides a novel strategy to design active sites of heterogeneous catalyst with synergetic catalysis.

2. Experimental section

2.1. Catalyst preparation

Pt catalysts loaded on different supports (ZSM-5, Al_2O_3, ZrO_2, CeO_2) were prepared by wetness impregnation method as shown in Scheme 1. In typical, 1 g support was mixed with the desired amount of $Pt(NO_3)_2$ solution (0.002 g_{Pt}·mL^{-1}, 5 mL) and stirred under room temperature for 2 hours. Afterwards, the mixture was evaporated by water bath at 90 °C to obtained dry power, and then the power was calcined with a heating rate of 10 °C min^{-1} to 500 °C in muffle furance for 4 hours. The parent supported Pt catalysts were obtained and denoted to Pt/ZSM-5, Pt/Al_2O_3, Pt/ZrO_2 and Pt/CeO_2 catalyst, respectively.

The as-prepared supported Pt catalyst was sulfate modified by in situ pyrolysis of $(NH_4)_2SO_4$ mixed with catalyst as shown in Scheme 1. For instance, 1 g as-prepared supported Pt catalyst power and the desired amount of $(NH_4)_2SO_4$ solid was ground and evenly mixed. Subsequently, the solid mixture was calcined in muffle furnace at 550 °C for 3 hours. Taking Pt/ZSM-5 catalyst as example, the finally obtained sulfate modified catalyst was denoted to xS-yPt/ZSM-5 (x represents the mass percentage of $(NH_4)_2SO_4$ to Pt based catalyst, y is the Pt weight percentage in catalyst), for instance, 5S-2Pt/ZSM-5 refers 0.05 g $(NH_4)_2SO_4$ is used for treating 1 g 2Pt/ZSM-5 catalyst.

2.2. Characterization

The crystalline phase of as-prepared these catalysts was characterized by powder X-ray diffraction (XRD) patterns on a Bruker D8 diffractometer using the Cu Kα radiation operating at 40 kV and 40 mA with a scan speed of 12° min^{-1} in the 2θ range of 10–90°. The actual Pt and S contents in these Pt based catalysts were measured by X-ray fluorescence (XRF) using the Shimadzu XRF-1800 spectrometer. Brunauer-Emmet-Teller (BET) surface area of the catalyst was determined by nitrogen adsorption at 77 K on a BK 200 C apparatus. Prior the test, the catalyst was degassed at 100 °C for 4 hours. To measure the CO chemisorption uptake, the catalyst was firstly pre-reduced under a mixture gas flow (5%H_2+95%He, 30 mL min^{-1}) at 150 °C for 1 hour. Afterwards, the pulse CO chemisorption was tested on a BELCAT II analyzer, with the assumption of CO: Pt=1:1. Hydrogen temperature-programmed reduction (H_2-TPR) experiment was conducted to test the reduction property of catalyst. In typical, 50 mg of catalyst pre-treated by drying at 100 °C for 12 hours was put in the reactor and heated from 30 to 800 °C with a heating ramp of 20 °C min^{-1} (in a flow of 5% H_2 + 95% N_2, 30 mL min^{-1}). NH_3-temperature programmed desorption (NH_3-TPD) experiment was preformed on the self-made tubular quartz reactor equipped with a thermal conductivity detector (TCD). Prior to the test, the catalyst (200 mg, 60–80 mesh) was put in the reactor and pre-treated in a N_2 flow (20 mL min^{-1}) under 300 °C for 0.5 h, and cooled down to 50 °C. Then, high purity NH_3 gas was flowed in the reactor (30 mL min^{-1}) for 10 min, and N_2 flow (20 mL min^{-1}) was purged for 0.5 h to clean the gaseous or physically adsorbed NH_3 on catalyst. Then, the catalysts were heated from 40 to 700 °C in a high purity N_2 flow (20 mL min^{-1}) to desorb the chemical adsorption NH_3, and outlet gas from the reactor was dehydrated by KOH and then introduced into TCD detector to record the NH_3 signal. The relative NH_3 desorption amount was calculated by fitting desorption peak area. X-ray photoelectron spectra (XPS) were recorded using an ESCALAB 250Xi instrument with Al Kα source ($h\nu$= 1484.6 eV) and the bind energy was calibrated by Si 2p (Eb = 103.4 eV).

2.3. Catalytic activity evaluation

Propane combustion reaction was conducted in a home-made fixed

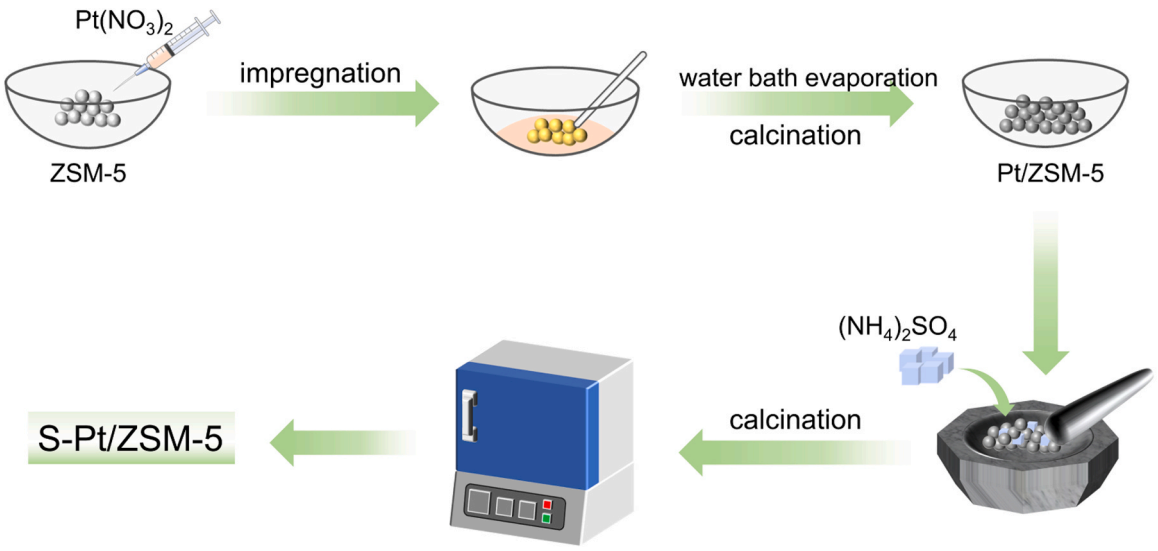

Scheme 1. Preparation diagram of Pt/ZSM-5 and S-Pt/ZSM-5 catalyst.

bed. In typical, the as-prepared catalyst (50 mg, 60–80 mesh) with quartz wool was put into a quartz tube with a inside diameter of 6 mm. The reaction mixture gas of 0.2 vol%C_3H_8 + 2 vol%O_2/balanced by N_2 was flowed into the fixed bed with a rate of 66.66 mL min^{-1} (mass space velocity of 80 000 mL g^{-1} h^{-1}). To control the 5% water concentration in the feed gas, the propane mixture gas went through a water bottle (water vapor partial pressure of 5.03 kPa) at 33.4 °C. The reaction temperature was controlled by a temperature-programmed equipment. To analyze the propane conversion, the inlet and outlet gas of the fixed bed was determined by the Shimadzu GC-2014 gas chromatography, which was equipped with a FID detector and HPGS-GASPRO capillary column.

2.4. Catalytic reaction kinetics

Kinetic test of propane oxidation was conducted under a low propane conversion (<15%) to exclude the mass transfer and heat transfer effect. Specifically, the typical Weisz-Prater formula (CWP) can be applied to exclude the internal diffusion effects, while the Mears criterion (CM) is adopted to exclude both the external diffusion and heat transfer effects. Reaction orders of reaction gas (oxygen and propane) are measured under a controlled partial pressures (propane of 0.202–0.808 kPa, oxygen of 1.515–9.09 kPa). The apparent activation energy (Ea) of catalyst was obtained by studying the catalytic activity at different reaction temperature.

3. Result and discussion

3.1. Sulfate modified Pt catalysts for propane oxidation

Fig. 1 shows the XRD patterns of the parent catalysts (2Pt/ZrO_2, 2Pt/Al_2O_3, 2Pt/CeO_2, and 2Pt/ZSM-5) and the sulfate modified catalysts (5S-2Pt/ZrO_2, 5S-2Pt/Al_2O_3, 5S-2Pt/CeO_2, and 5S-2Pt/ZSM-5) to investigate whether catalyst structure changes during sulfate modification. For the 2Pt/ZSM-5 and 5S-2Pt/ZSM-5 catalysts, the characteristic diffraction peaks appearing at 7.9, 8.8, 23.2, 23.6 and 24.4° are observed, which are assigned to MIF structure of ZSM-5 support (JCPDS No. 44–0002) [44,45]. This result suggests that the bulk structure of ZSM-5 support is remained after sulfate modification. Besides, new diffraction peaks at 39.7, 46.2, and 67.7° are found for the 5S-2Pt/ZSM-5 catalyst compared to 2Pt/ZSM-5, attributed to the diffraction peaks of (111), (200) and (220) facets of the cubic metallic Pt (JCPDS No. 04–0802). This result indicates the growth of the Pt nanoparticles during sulfate modification. To observe the Pt nanoparticles on catalyst, the HRTEM images of the representative 5S-2Pt/ZSM-5 and 2Pt/ZSM-5 catalysts are measured as shown in Fig. 2. It can be seen that the Pt nanoparticles on 5S-2Pt/ZSM-5 catalyst is slightly larger than that on 2Pt/ZSM-5 catalyst. And the element-mapping of 5S-2Pt/ZSM-5 catalyst indicates the S element is uniformly distributed in the 5S-2Pt/ZSM-5 catalyst. For the 2Pt/ZrO_2 and 5S-2Pt/ZrO_2 catalysts, the characteristic diffraction peaks observed at 24.4, 28.2, 31.5, 34.2, 35.3, 49.3 and 50.1° correspond to the monoclinic ZrO_2 (m-ZrO_2, JCPDS No. 37–1484) [46]. For the 2Pt/Al_2O_3 and 5S-2Pt/Al_2O_3 catalysts, the characteristic diffraction peaks observed at 32.8, 36.8, 39.8, 45.7, 61.0, 67.1 and 85.0° are assigned to the Al_2O_3 support (JCPDS No. 50-0741) [47]. For the 2Pt/CeO_2 and 5S-2Pt/CeO_2 catalysts, the characteristic diffraction peaks appearing at 28.7, 33.2, 47.7, 56.5, 59.3, 69.6, 76.9 and 79.4° are attributed to the CeO_2 cubic fluorite structure (JCPDS No. 34–0394) [48]. Besides the 5S-2Pt/ZSM-5 catalyst, no evident characteristic peak assigned to Pt species is observed for 5S-2Pt/ZrO_2, 5S-2Pt/Al_2O_3 and 5S-2Pt/CeO_2 catalysts, suggesting the growth of Pt nanoparticles is not significant in these catalysts. Table 1 summaries the surface area of these catalysts, 2Pt/ZSM-5 catalyst exhibits the highest surface area among them, the 2Pt/Al_2O_3 catalyst gives the moderate high surface area. Additionally, it can be seen that these sulfate modified Pt catalysts show lower surface area compared to their parent catalyst, the decrease surface area can be ascribed to the catalyst pore collapsing due to heat treatment during sulfate modified process.

Fig. 3 shows the catalytic activities of parent and sulfate modified Pt catalysts for propane oxidation. Compared to the parent Pt catalyst, the sulfate modified Pt catalyst loaded on different supports exhibit much higher catalytic activity for propane complete oxidation. For instance, the 5S-2Pt/ZrO_2 catalyst gives a much lower T_{80} of 215 °C in comparison with that of 300 °C for the 2Pt/ZrO_2 catalyst. T_{80} of 2Pt/Al_2O_3 catalyst decreases from 330 to 220 °C after sulfate modification, T_{80} of 2Pt/CeO_2 catalyst decreases from 390 to 340 °C after sulfate modification. The T_{80} of 2Pt/ZSM-5 catalyst decreases from 250 to 210 °C. The above results confirm the significant promotion of sulfate modification on these Pt catalysts for propane oxidation. Table 2 also lists the specific mass reaction rate and T_{80} of these catalysts for propane oxidation. The 5S-2Pt/ZSM-5 catalyst exhibits the highest specific mass reaction of 1.9 $\mu mol \cdot g_{cat}^{-1} \cdot s^{-1}$ among these catalysts, which further confirms the superior catalytic activity of the 5S-2Pt/ZSM-5 catalyst. Besides, most works focused on the sulfate modification on single oxides (Pt/Al_2O_3, Pt/CeO_2 and Pt/ZrO_2) [29,30,43,56] supported Pt, the studies on the sulfate modification of the Pt/ZSM-5, one of the most important heterogeneous catalysts for propane oxidation, are scarcely reported. The behavior of

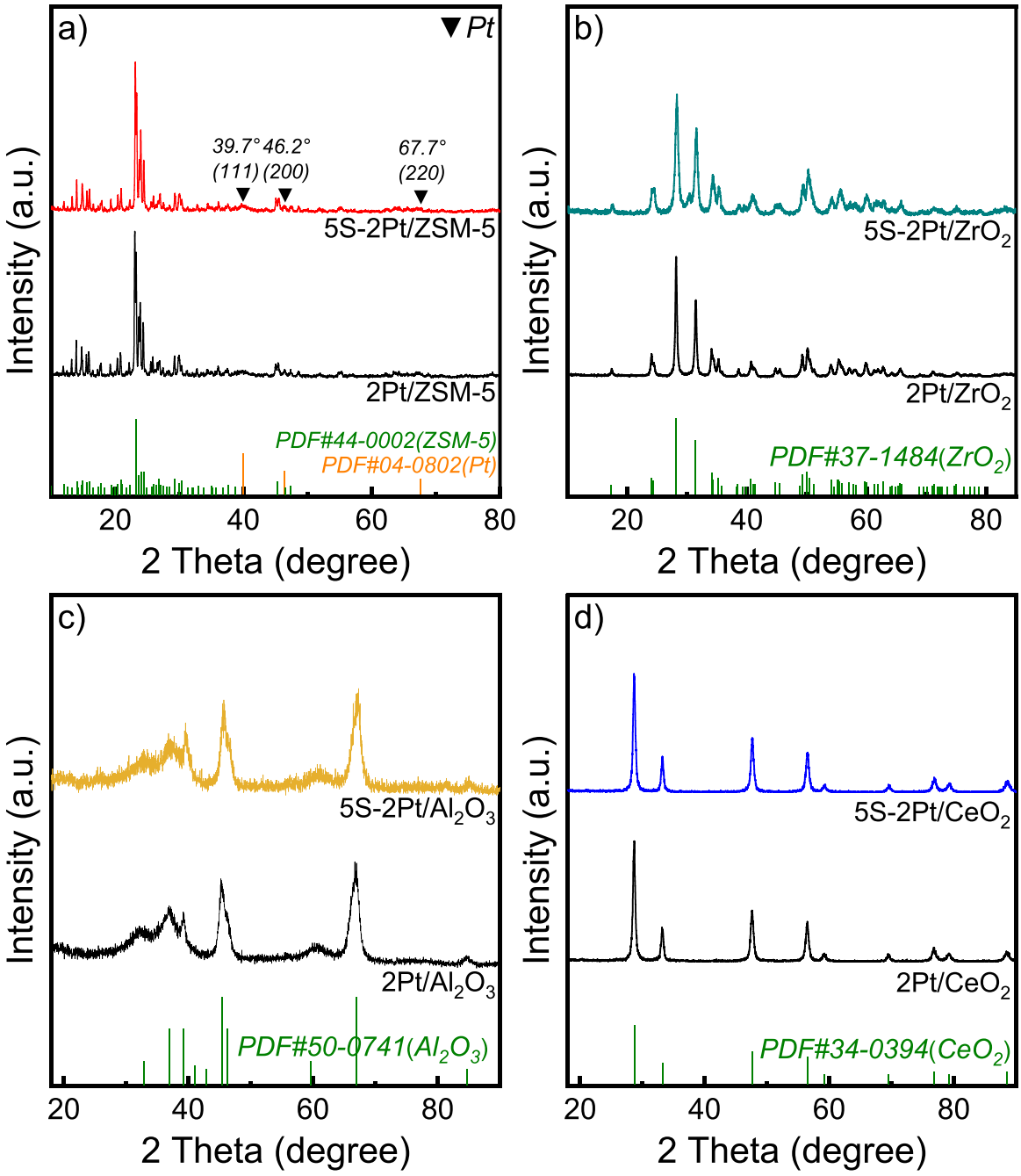

Fig. 1. XRD patterns of parent Pt based catalysts and the sulfate modified Pt catalysts with different support: a) 2Pt/ZSM-5 and 5S-2Pt/ZSM-5, b) 2Pt/ZrO_2 and 5S-2Pt/ZrO_2, c) 2Pt/Al_2O_3 and 5S-2Pt/Al_2O_3 and d) 2Pt/CeO_2 and 5S-2Pt/CeO_2.

sulfate modification on Pt/ZSM-5 and its influence on catalytic are still lack of systematic research. Therefore, the following investigation focuses on deeply understanding the promotion of sulfate on the 2Pt/ZSM-5 catalyst.

3.2. Effect of sulfate content in Pt/ZSM-5 catalyst

To further optimize catalytic performance of sulfate modified 2Pt/ZSM-5 catalyst, the 2Pt/ZSM-5 catalysts modified with different sulfate content were prepared by adjusting $(NH_4)_2SO_4$ amount. Fig. 4 and Figure S1 shows the characterizations and catalytic activity of these sulfate modified 2Pt/ZSM-5 catalysts. In Fig. 4a, it can be seen that all these S-2Pt/ZSM-5 catalysts show the characteristic diffraction peaks assigned to the ZSM-5 support (JCPDS No. 44–0002), indicating the well-remained structure of the ZSM-5 support during the sulfate modification. Interestingly, the characteristic diffraction peaks at 39.7, 46.2, and 67.7° attributed to (111), (200) and (220) facets of Pt species (JCPDS No. 04–0802) are not observed for 2Pt/ZSM-5 catalyst but gradually increase for 2S-2Pt/ZSM-5 and 5S-2Pt/ZSM-5 catalysts, particularly for the 100S-2Pt/ZSM-5 catalyst with very strong these peaks. Such result suggests the increase of sulfate content in modification leads to the gradual growth of Pt particles but not affects the structure of ZSM-5. Fig. 4b displays the NH_3-TPD profiles of the sulfate modified Pt/ZSM-5 catalysts, the strong NH_3 desorption peaks of the Pt/ZSM-5 catalyst suggests its abundant acid sites, but the NH_3 desorption peak area does not change remarkably with the increase of sulfate content during modification process, and the relative surface acidity for these catalyst only slightly increase when $(NH_4)_2SO_4$. Such result may be

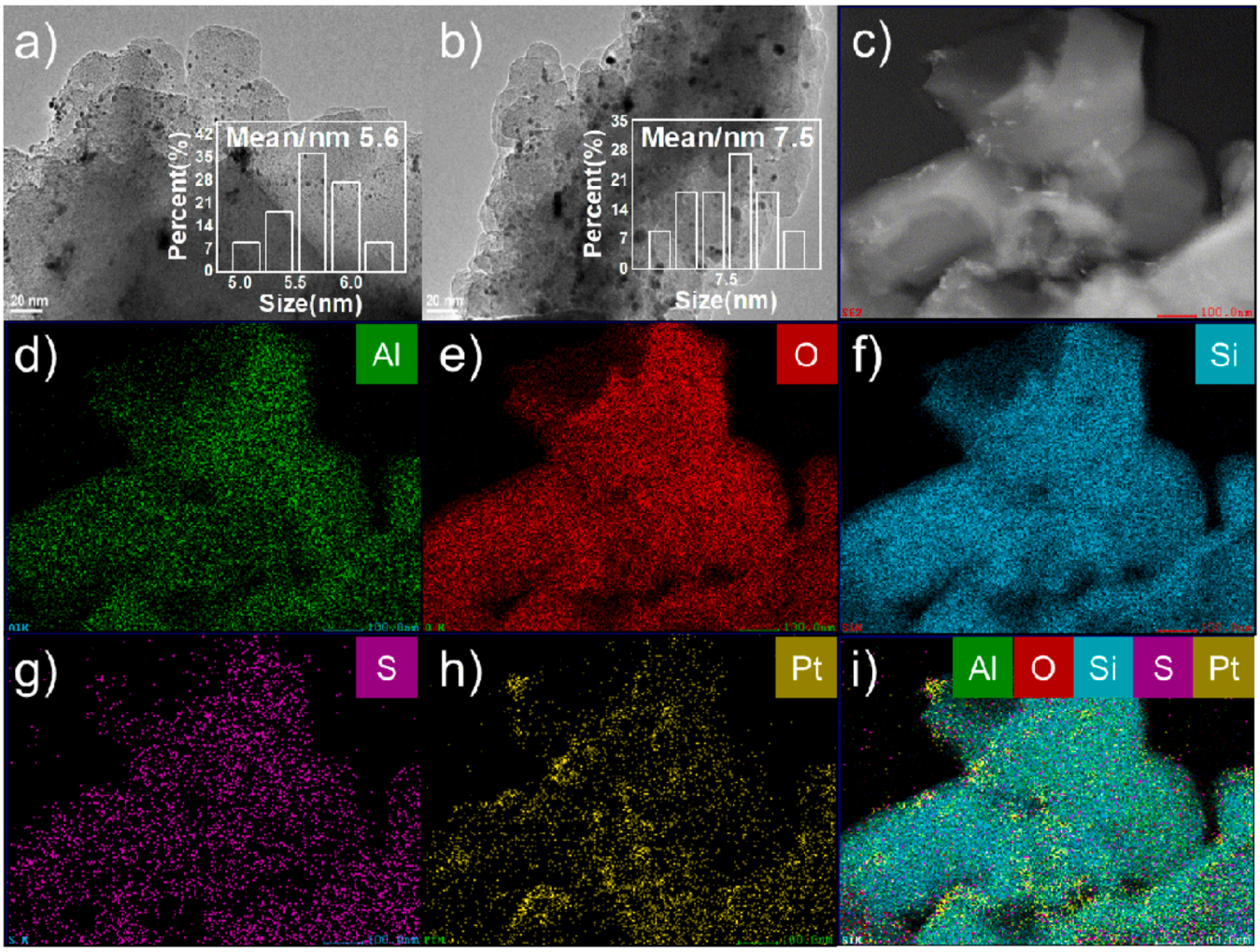

Fig. 2. The HRTEM images of a) 2Pt/ZSM-5 and b) 5S-2Pt/ZSM-5 catalysts (with the images of Pt nanoparticles size distribution inserted), c-i) Element-mapping analysis of 5S-2Pt/ZSM-5 catalyst.

Table 1
Surface area of these Pt catalysts before and after sulfate modified.

BET surface area[a] / $m^2 \cdot g^{-1}$			
2Pt/ZSM-5	341	5S-2Pt/ZSM-5	302
2Pt/ZrO_2	75	5S-2Pt/ZrO_2	48
2Pt/Al_2O_3	103	5S-2Pt/Al_2O_3	76
2Pt/CeO_2	51	5S-2Pt/CeO_2	46

[a] The BET surface area was determined by N_2 adsorption.

ascribed to the limited amount sulfate actually modified in the Pt/ZSM-5 catalyst, as confirmed by S content measurement discussed in following. The pyridine-IR spectra of three representative catalysts of 2Pt/ZSM-5, 2S-2Pt/ZSM-5 and 5S-2Pt/ZSM-5 catalysts were carried out to study the type of acid sites as shown in Figure S2. The vibration peaks at 1540 cm^{-1} is ascribed to pyridine adsorbed on Bronsted acid site, while the vibration peaks at 1450 cm^{-1} corresponds to pyridine adsorbed on Lewis acid site [49,50]. It can be found that both Bronsted acid site and Lewis acid site exist on the catalyst surface. And sulfate modification may slightly increase the Lewis acid site, which is confirmed by the change of relative intensity of peak regarding Bronsted acid site and Lewis acid site (Figure S2). The H_2-TPR profiles are also measured to study the reducibility of the sulfate modified catalysts as shown in Fig. 4c. For the 5 S/ZSM-5 sample, a reduction peak with H_2 consumption of 0.05 mmol g_{cat}^{-1} appearing at 500 °C is assigned to the reduction of sulfate species on the ZSM-5 support, such reduction behavior becomes more remarkable for the 100 S/ZSM-5 treated with more sulfate substance, exhibiting a H_2 consumption of 1.36 mmol g_{cat}^{-1}. This result confirms the sulfate specie can be decorated on the ZSM-5 surface, and the loaded sulfate amount on ZSM-5 may increase with the increase of the $(NH_4)_2SO_4$ amount during modification for ZSM-5 support. For the 2Pt/ZSM-5 catalyst, the H_2 consumption peak at 160 and 360 °C is assigned to the reduction of easily reduced PtO_x species and support strongly interacted PtO_x species, respectively; and the related total amount of H_2 consumption is 0.88 mmol g_{cat}^{-1}. After sulfate modification, the reduction peaks shift to higher temperature for the sulfate modified Pt/ZSM-5 catalyst, suggesting that the PtO_x species become more stable and difficult to be reduced. This result may be assigned to the strong interaction between PtO_x and sulfate species. Due to the H_2 consumption by sulfate species, 2S-2Pt/ZSM-5 catalyst shows much higher H_2 consumption of 1.59 mmol g_{cat}^{-1} compared to the 2Pt/ZSM-5 catalyst (1.36 mmol g_{cat}^{-1}). Surprisingly, the H_2 consumption of the 5S-2Pt/ZSM-5 catalyst only slightly increase to 1.67 mmol g_{cat}^{-1}, and the 100S-2Pt/ZSM-5 catalyst shows a comparable H_2 consumption with the 5S-2Pt/ZSM-5 catalyst. To explain such result, the S content of these catalyst is analyzed and listed in Table 3. It is found that the tendency of sulfate content increase in 2Pt/ZSM-5 is very different with that of ZSM-5, namely, sulfate in ZSM-5 support is positively correlated with the used $(NH_4)_2SO_4$. Whereas, sulfate content in those sulfate modified 2Pt/ZSM-5 catalysts firstly increases then keeps constant when

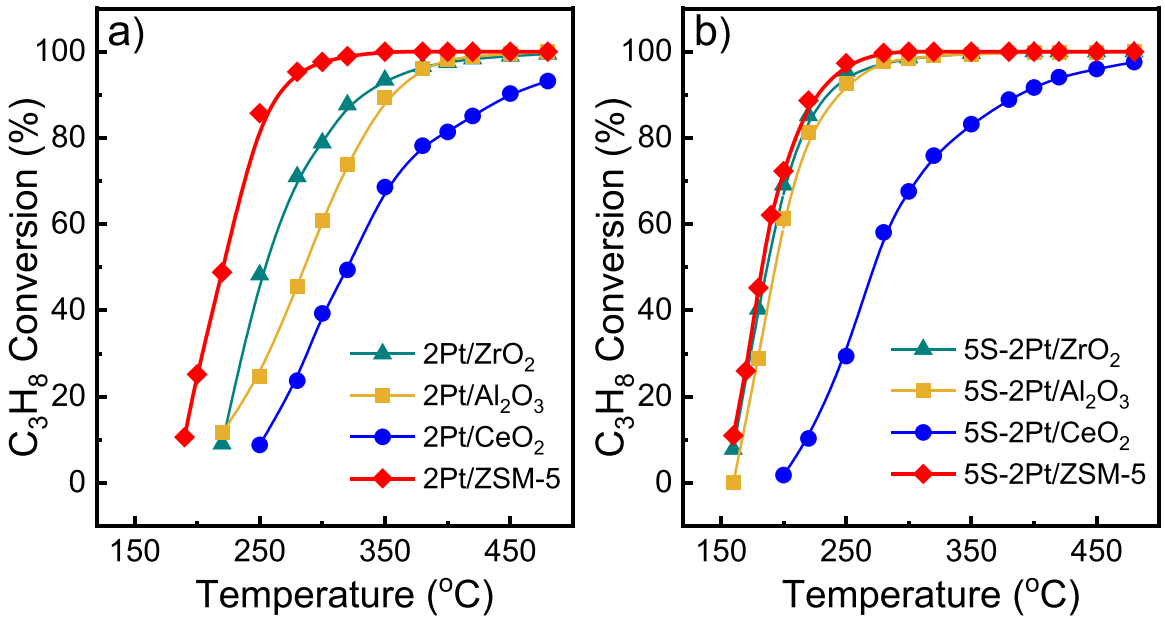

Fig. 3. The light-off curves of propane oxidation over parent Pt based catalysts and the sulfate modified Pt catalysts loaded on different support.

Table 2
Specific mass reaction rate and T_{80} of parent Pt based catalysts and the sulfate modified Pt catalysts for propane combustion.

Catalyst	Specific mass reaction rate[a] / μmol·g_{cat}^{-1}·s^{-1}		T_{80}[b] /°C		△T[c]/°C
	r_1	r_2	T_1	T_2	
2Pt/ZSM-5	1.5	1.9	250	210	40
2Pt/ZrO_2	1.1	1.8	300	215	85
2Pt/Al_2O_3	0.6	1.8	330	220	110
2Pt/CeO_2	0.3	0.8	390	340	50

[a] r_1 represents the reaction rate for parent catalyst at 220 °C, r_2 represents the reaction rate for sulfate modified catalyst at 220 °C;
[b] The temperature for propane conversion of 80%, T_1 represents the temperature for parent catalyst, T_2 represents the temperature for sulfate modified catalyst;
[c] $\triangle T = T_1 - T_2$.

$(NH_4)_2SO_4$ amount increased. For instance, 5S-2Pt/ZSM-5 shows higher S content than 2S-2Pt/ZSM-5 but comparable S content to the 100S-2Pt/ZSM-5 catalyst. Such result indicates the existence of Pt species would control the amount of S accumulation in S-2Pt/ZSM-5, suggesting the Pt species interacts with sulfate. The catalytic activity of these catalysts for propane oxidation is also evaluated in Fig. 4d. Sulfate on parent ZSM-5 hardly promotes propane oxidation reaction as evidenced by 5 S/ZSM-5 activity. Whereas, the catalytic activity of sulfate modified S-2Pt/ZSM-5 catalyst increases firstly and then remains unchanged when the $(NH_4)_2SO_4$ amount increases. This result suggests sulfate enhances the Pt/ZSM-5 catalyst activity and only suitable sulfate content in the Pt/ZSM-5 catalyst leads to the highest catalytic activity.

3.3. Role of Pt/S atomic ratio in sulfate modified Pt/ZSM-5 catalyst

To further investigate the influence of sulfate on Pt/ZSM-5 catalyst, the role of Pt/S atomic ratio in sulfate modified Pt/ZSM-5 catalyst on catalytic performance has been studied in detail. Given that modified sulfate in 2Pt/ZSM-5 catalyst is nearly constant amount when $(NH_4)_2SO_4$ amount increased over 5 wt% of 2Pt/ZSM-5 (Table 3), the Pt loading was changed to achieve the Pt/ZSM-5 catalyst with different Pt/S atomic ratio. Table 4 lists the corresponding physical physical-chemical parameters of sulfate modified Pt/ZSM-5 catalyst with different Pt loading. It can be found that the uptake of CO chemical adsorption increases with the increase of Pt loading, suggesting the total exposed Pt atoms increases when Pt loading increases. All these catalysts show very high BET surface area, indicating the well remained ZSM-5 porous structure. The actual contents of Pt and S element are measured by XRF and provided in Table 4. It is found that the content of Pt is nearly consistent with the theoretical value due to the wetness impregnation method used. It is found that S content in 5S-yPt/ZSM-5 firstly increases then decreases when Pt content increases from 0 to 3 wt%. For instance, the 5 S/ZSM-5 has S content of 0.06 wt%, while the 5S-1Pt/ZSM-5 contains S content of 0.73 wt%. S content will decrease to 0.64 wt% when Pt content further increases to 3 wt% as observed in 5S-3Pt/ZSM-5. Therefore, it is worth noting that the presence of Pt also inhibits the excessive increase of S content. Especially for 100 S/ZSM-5, the S content decreases from 1.8 to 0.7 wt% when Pt loaded to 2 wt% as observed in 100S-2Pt/ZSM-5. Thus, it is inferred that Pt specie promotes the increase of sulfate when sulfate is low content, however, Pt species also boosts the sulfate decomposition when the S content is excessive or the Pt content is high. As shown in Table 4, the gradual increase tendency of Pt/S atomic ratio has been successfully achieved for these sulfate modified 5S-Pt/ZSM-5 catalyst with different Pt loading.

Fig. 5 shows the catalytic activities of the parent and sulfate modified Pt/ZSM-5 catalysts with various Pt loading. For the parent Pt/ZSM-5 catalyst, the activity slightly increase when Pt loading increases. However, the activity of the sulfate modified Pt/ZSM-5 catalyst remarkably increase when Pt loading increases from 0 to 2 wt% as show in Fig. 5a. This result suggests introduction of sulfate species significantly affects the catalytic behavior of the Pt/ZSM-5 catalyst. The 5S-3Pt/ZSM-5 catalyst exhibits the comparable activity to that of 5S-2Pt/ZSM-5 catalyst at same reaction temperature, indicating the Pt species optimal loading of 2 wt% to achieve the highest catalytic activity. In viewpoint of Pt atom utilization efficiency, it is necessary to consider the specific mass reaction rate per gramme Pt in catalyst and its relationship regarding Pt/S atomic ratio. It can be found that the relationship between Pt/S atomic ratio and specific mass rate presents a volcano curve in Fig. 5b, namely specific mass rate firstly increase then decrease when the Pt/S atomic ratio increases. Such result confirms that the 5S-2Pt/ZSM-5 with Pt/S atomic ratio of 0.5 achieves the highest efficiency of Pt atom utilization. And the specific mass reaction rate of 5S-2Pt/ZSM-5 (86.5 μmol·g_{Pt}^{-1}·s^{-1}) is much higher than previous works as listed in Table S2.

To deeply understand the sulfate promotion on Pt/ZSM-5 catalyst,

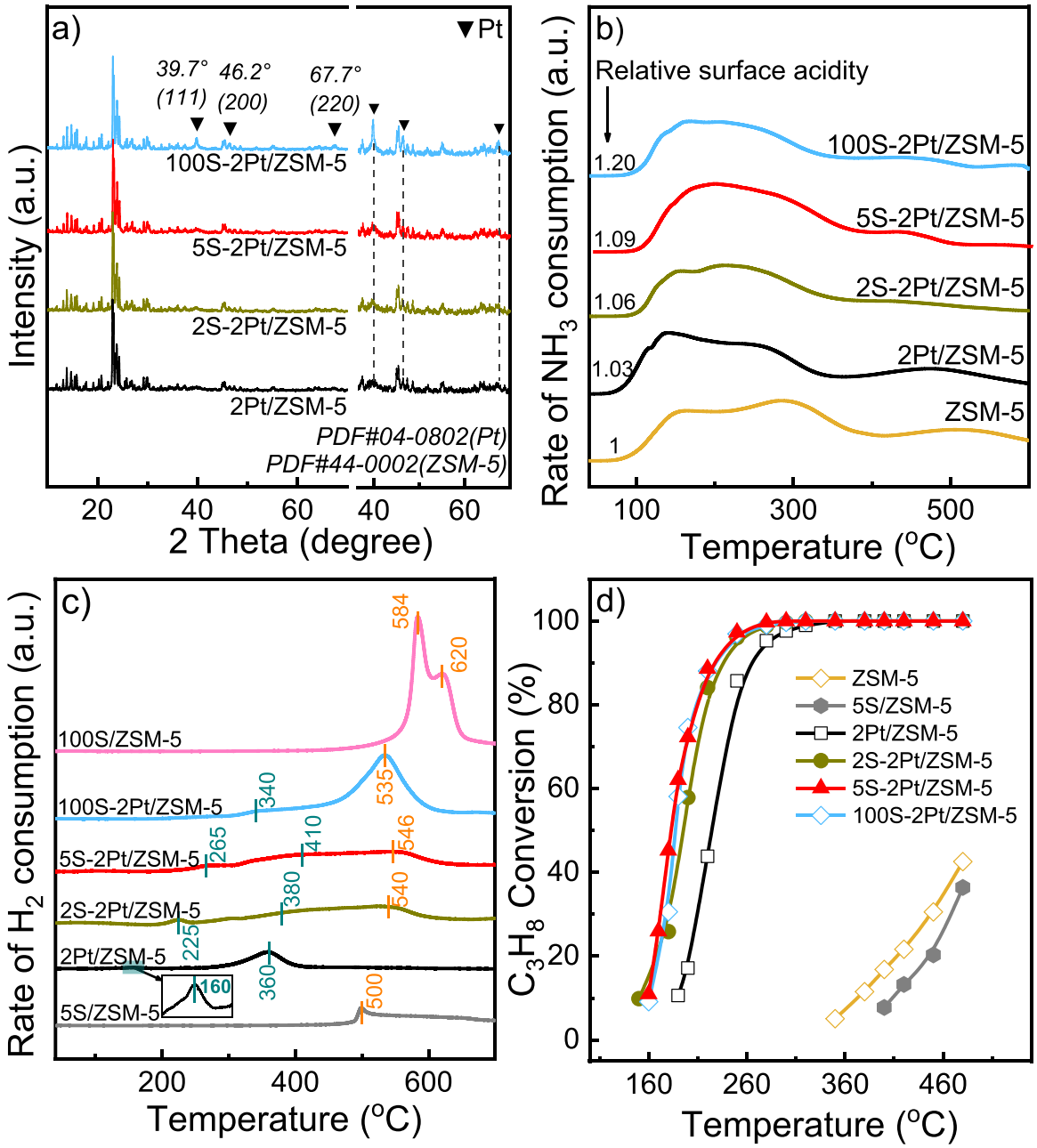

Fig. 4. a) XRD patterns, b) NH_3-TPD, c) H_2-TPR profiles and d) The light-off curves of propane oxidation of the sulfate modified Pt/ZSM-5 catalysts.

the CO chemical adsorption of the representative sulfate modified Pt/ZSM-5 catalysts (5S-0.5Pt/ZSM-5, 5S-1Pt/ZSM-5, 5S-2Pt/ZSM-5 and 5S-3Pt/ZSM-5) was analyzed, the CO chemical uptake of parent Pt/ZSM-5 catalyst is listed in the Table S1. The Pt/S atomic ratio of these catalysts is increased from 0.1 to 0.7 as shown in Table 4. The 0.5Pt/ZSM-5, 1Pt/ZSM-5, 2Pt/ZSM-5 and 3Pt/ZSM-5 catalyst shows CO uptake of 7.0, 15.1, 18.4 and 26.3 μmol·g^{-1}, respectively. In comparison, the 5S-0.5Pt/ZSM-5, 5S-1Pt/ZSM-5, 5S-2Pt/ZSM-5 and 5S-3Pt/ZSM-5 catalyst gives CO uptake of 1.4, 5.8, 9.6 and 17.1 μmol·g^{-1}, respectively. The CO uptake of sulfate modified Pt/ZSM-5 catalyst decreases compared to the corresponding parent Pt/ZSM-5 catalyst, the decrease extent of CO uptake gradually decrease when Pt/S atomic ratio increases. For instance, near 80% CO uptake decreases for the 5S-0.5Pt/ZSM-5 catalyst compared to the 0.5Pt/ZSM-5 catalyst, but only 35% CO uptake decreases for the 5S-3Pt/ZSM-5 catalyst compared to the 3Pt/ZSM-5 catalyst. The CO uptake decrease of sulfate modified Pt/ZSM-5 catalyst should be mainly ascribed to the strong interaction between Pt species and sulfate species, which is discussed for Pt/ZrO_2 and sulfate modified Pt/ZrO_2 in our previous work [43], although Pt nanoparticles size slightly increases for sulfate modified Pt/ZSM-5 catalyst. Thus, the relative strength of Pt species and sulfate interaction can be evaluated based on the CO chemical uptake change for these catalysts. For instance, the 5S-3Pt/ZSM-5 catalyst shows the lowest extent (35%) of CO uptake decrease among these sulfate modified catalysts, suggesting the weakest strength of Pt species and sulfate interaction. The relative strength of Pt species and sulfate interaction in other sulfate modified catalyst is calculated by comparing the decrease extent of CO uptake to the 5S-3Pt/ZSM-5 catalyst, as described in the formula (1). The 5S-0.5Pt/ZSM-5 catalyst (with 80% CO uptake decrease) exhibits relative strength of interaction between Pt species and sulfate species of 2.3 in comparison with the 5S-3Pt/ZSM-5 catalyst. The relationship between specific mass reaction and relative strength of interaction

Table 3
The physical-chemical parameters of parent and the sulfate modified Pt/ZSM-5 catalysts.

Catalyst	CO uptake[a] / μmol g^{-1}	Pt dispersion[b] / %	Pt average size[b] / nm	BET surface area[c] / $m^2 \cdot g^{-1}$	Element content[d]				H_2 consumption[e] / °C	H_2 mmol $\cdot g_{cat}^{-1}$
					Pt		S			
					wt %	mmol g^{-1}	wt %	mmol g^{-1}		
5 S/ZSM-5	0	0	0	345	-	-	0.06	0.018	-	0.05
2Pt/ZSM-5	18.4	17.9	6.3	341	1.8	0.092	0	0	246	0.88
2S-2Pt/ZSM-5	16.0	15.6	7.3	328	1.8	0.092	0.3	0.094	220	1.59
5S-2Pt/ZSM-5	9.6	9.4	12.1	302	1.8	0.092	0.7	0.219	210	1.67
100S-2Pt/ZSM-5	5.8	5.6	20.1	310	1.7	0.087	0.7	0.219	214	1.68
100 S/ZSM-5	0	0	0	315	-	-	1.8	0.563	-	1.36

[a] The CO uptake was tested by chemical CO pulse adsorption;
[b] Pt dispersion and Pt average size were determined by CO chemisorption;
[c] The BET surface area was determined by N_2 adsorption;
[d] The Pt content was measure by XRF;
[e] The H_2 consumption was measured by H_2-TPR and calibrated by the CuO.

Table 4
The physical-chemical parameters of parent Pt/ZSM-5 based catalysts and the sulfate modified Pt/ZSM-5 catalysts.

Catalyst	CO uptake[a] / μmol·g^{-1}	Pt dispersion[b] / %	Pt average size[b] / nm	BET surface area[c] / $m^2 \cdot g^{-1}$	Element content[d]				Pt/S atomic ratio	Specific mass reaction rate[e] / μmol·$g_{Pt}^{-1} \cdot s^{-1}$	H_2 consumption[f] / mmol·g_{cat}^{-1}
					Pt		S				
					(wt %)	(mmol/g)	(wt %)	(mmol/g)			
5 S/ZSM-5	0	0	0	345	0	0	0.06	0.018	0	-	0.05
5S-0.5Pt/ZSM-5	1.4	5.5	20.6	335	0.5	0.026	0.71	0.22	0.1	60.2	-
5S-1Pt/ZSM-5	5.8	6.4	17.2	327	0.9	0.046	0.73	0.23	0.2	68.9	-
5S-2Pt/ZSM-5	9.6	9.4	12.1	322	1.8	0.092	0.67	0.20	0.5	86.5	1.67
5S-3Pt/ZSM-5	17.1	11.1	10.2	315	2.6	0.133	0.64	0.20	0.7	70.7	-

[a] The CO uptake was tested by chemical CO pulse adsorption;
[b] Pt dispersion and Pt average size were determined by CO chemisorption;
[c] The BET surface area was determined by N_2 adsorption;
[d] The Pt and S content was measure by XRF;
[e] The specific mass reaction rate was determined at 200 °C;
[f] The H_2 consumption was measured by H_2-TPR and calibrated by the CuO.

(between Pt species and sulfate species) is constructed as shown in Fig. 5e. It can be inferred that only suitable strength of Pt species and sulfate interaction leads to their optimizing synergetic catalysis and highest catalytic activity.

$$\mathrm{RelativestrengthofPtandSinteraction} = \frac{1-\frac{a}{b}}{c} \quad (1)$$

a represents the CO uptake of sulfate modified Pt/ZSM-5 (5S-0.5Pt/ZSM-5, 5S-1Pt/ZSM-5, 5S-2Pt/ZSM-5 and 5S-3Pt/ZSM-5), *b* represents the CO uptake of the corresponding parent Pt/ZSM-5 (0.5Pt/ZSM-5, 1Pt/ZSM-5, 2Pt/ZSM-5 and 3Pt/ZSM-5), *c* represents the CO uptake decrease (35%) of the 5S-3Pt/ZSM-5 catalyst compared to the 3Pt/ZSM-5 catalyst because of its minimum CO uptake decrease.

3.4. Kinetic result

To deeply understand the difference of catalytic behaviors between parent Pt/ZSM-5 and sulfate modified Pt/ZSM-5 catalyst, kinetic experiments of propane oxidation over two representative 2Pt/ZSM-5 and 5S-2Pt/ZSM-5 catalysts are conducted as shown in Fig. 6. The reaction rates of both the 2Pt/ZSM-5 and 5S-2Pt/ZSM-5 catalysts increase with the increase of propane or oxygen partial pressure. Propane usually presents weak adsorption on the catalyst surface thus propane reaction order observed close to one is consistent with the previous works [43]. Oxygen often exhibits strong adsorption on noble metal catalyst, and the saturated adsorption of oxygen is observed for the 2Pt/ZSM-5 and 5S-2Pt/ZSM-5 catalysts. The derived power law rate expressions are $r = 1.7 \times 10^{-6}[C_3H_8]^1[O_2]^{0.25}$ for the 2Pt/ZSM-5 catalyst, and $r = 4.3 \times 10^{-6}[C_3H_8]^{1.03}[O_2]^{0.17}$ for the 5S-2Pt/ZSM-5 catalyst, and the related kinetic parameters are summarized in Table 5. Much higher apparent rate constant *k* obtained on the 5S-2Pt/ZSM-5 catalyst confirms its superior catalytic activity for propane oxidation compared to the 2Pt/ZSM-5 catalyst. This observation is consistent with apparent reactivity in the light-off curves (Fig. 5b). The apparent activation energy (Ea) of the 5S-2Pt/ZSM-5 catalyst (Ea = 55.8 kJ·mol^{-1}) is much lower than that of the 2Pt/ZSM-5 catalyst (Ea = 95.0 kJ·mol^{-1}). The remarkable decrease of Ea indicates the different reaction mechanism of propane oxidation over 2Pt/ZSM-5 and 5S-2Pt/ZSM-5 catalysts, which should be ascribed to the promotion of sulfate for propane activation, which further confirms the synergetic catalysis of Pt species and sulfate significantly promoting propane activation.

Previous works pointed out that sulfate species benefits the activation of C-C bonds in propane, thus enhancing the oxidation activity of catalyst [51,52]. For instance, Hinz *et al.* found the main route of

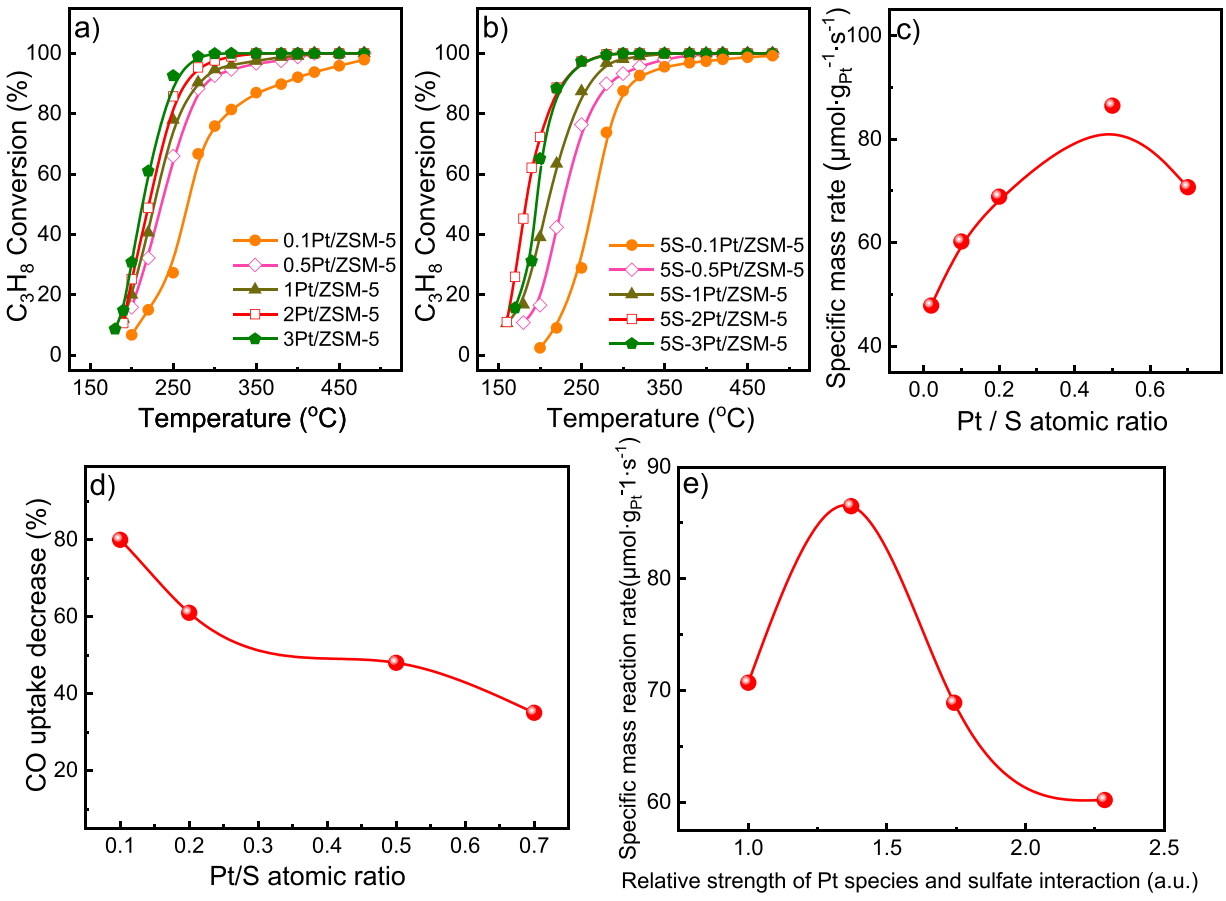

Fig. 5. a) The light off curves of 0.1Pt/ZSM-5, 0.5Pt/ZSM-5, 1Pt/ZSM-5, 2Pt/ZSM-5 and 3Pt/ZSM-5 catalyst for propane oxidation, b) The light off curves of 5S-0.1Pt/ZSM-5, 5S-0.5Pt/ZSM-5, 5S-1Pt/ZSM-5, 5S-2Pt/ZSM-5 and 5S-3Pt/ZSM-5 catalyst for propane oxidation, c) The relationship between the Pt/S atomic ratio with the specific mass reaction rate, d) The relationship between the Pt/S atomic ratio with CO uptake decrease extent of sulfate Pt/ZSM-5 compared to parent Pt/ZSM-5 catalyst, e) The relationship between the relative strength of Pt and S interaction with the specific mass reaction rate of sulfate modified Pt/ZSM-5 catalysts.

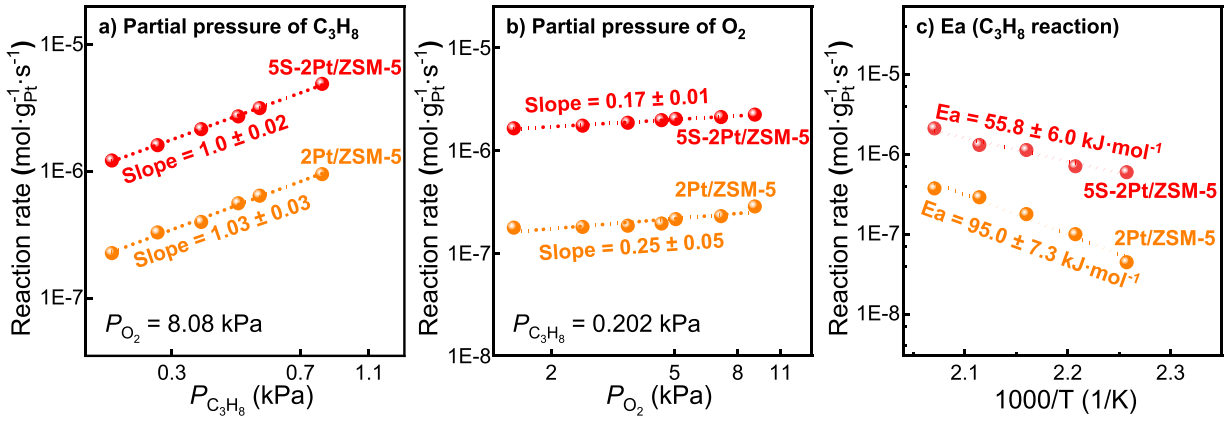

Fig. 6. Dependence of reaction rate on partial pressure of propane and oxygen, and Arrhenius plots of Pt/ZSM-5 catalysts.

Table 5
Kinetic parameters of propane oxidation over Pt/ZSM-5 and 5S-2Pt/ZSM-5 catalysts.

Catalyst	$r_{C3H8}=k_{app}[C_3H_8]^a[O_2]^b$			$E_{a(C3H8)}$ / kJ·mol^{-1}
	k_{app}/ $\times 10^{-6}$	a	b	
5S-2Pt/ZSM-5	4.3	1.0 ± 0.02	0.17 ± 0.01	55.8 ± 6.0
2Pt/ZSM-5	1.7	1.03 ± 0.03	0.25 ± 0.05	95.0 ± 7.3

propane complete oxidation in SO_2 promoted Pt/Al_2O_3 catalyst is the breaking of a C-C bond producing ethane and a C1 fragment, which then form CO and eventually CO_2 [52]. To clearly understand the reaction pathway in this work, the in situ DRIFT spectra of sequential C_3H_8, C_3H_8 + O_2 and N_2 purge over two representative catalysts (2Pt/ZSM-5 and 5S-2Pt/ZSM-5) at 250 °C were conducted (Fig. 7). For C_3H_8 purge step, the vibration peak at 2350 cm^{-1} accompanied by a inverted peak is attributed to the CO_2 signal observed for both 2Pt/ZSM-5 and 5S-2Pt/ZSM-5. In addition, the characteristic vibration peaks at 1424, 1558, and 1652 cm^{-1} is attributed to surface carbonate species on the

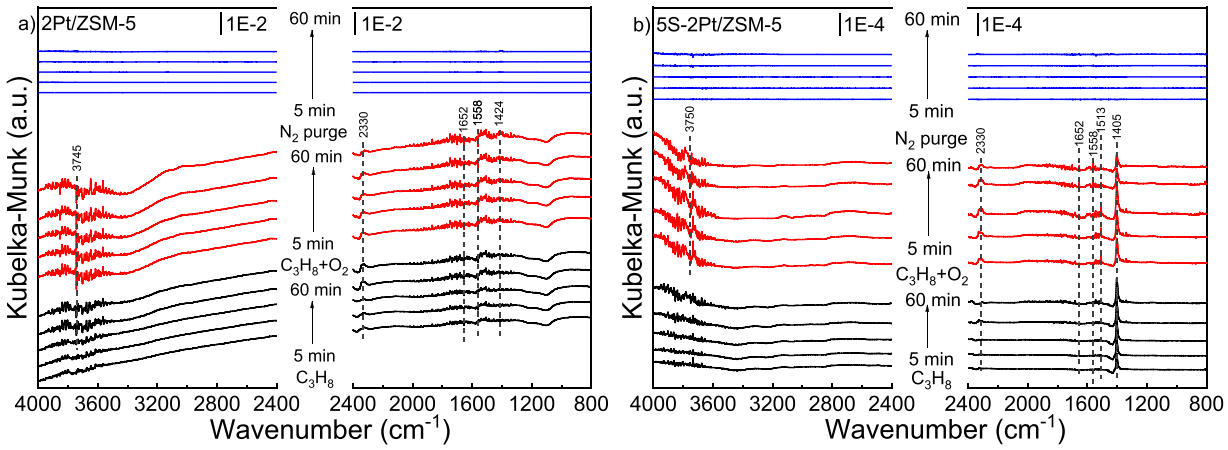

Fig. 7. In-situ DRIFT spectra of propane oxidation over a) 2Pt/ZSM-5 and b) 5S-2Pt/ZSM-5 catalysts at 250 °C.

2Pt/ZSM-5 catalyst. The above result indicates the propane oxidation reaction takes place on the 2Pt/ZSM-5 catalyst even though without O_2 in feed gas, which can be ascribed to surface active oxygen species existing on 2Pt/ZSM-5 catalyst surface. A very strong vibration peak can be observed at 1405 cm^{-1} for the 5S-2Pt/ZSM-5 catalyst, including those carbonate species at 1513, 1558, 1652 cm^{-1}. Such vibration peak (at 1405 cm^{-1}) is ascribed to the generation of enolate intermediates, as the powerful evidence of C-C bond crack during propane oxidation [42,53]. For C_3H_8 + O_2 purge step, a remarkable change can be found, namely, the vibration peak ascribed to enolate intermediates gradually decreases for the 5S-2Pt/ZSM-5 catalyst and the vibration peak ascribed to carbonate species slightly increases. This result suggests the gaseous O_2 in feed gas promotes the further oxidation of enolate intermediates. For N_2 purge step, those vibration peaks assigned to intermediates (carbonate species, enolate) disappear, confirming the intermediates on catalyst easily decompose during propane complete oxidation. To further distinguish the breaking of C-H bond and C-C bond by experiment, methane oxidation over two representative catalysts (5S-2Pt/ZSM-5 and 2Pt/ZSM-5) was conducted in Fig. 8a. It can be found that 5S-2Pt/ZSM-5 catalyst shows inferior catalytic activity for methane oxidation compared to parent 2Pt/ZSM-5 catalyst. This result suggests the C-H activation ability of 5S-2Pt/ZSM-5 catalyst is weaken compared to the parent 2Pt/ZSM-5 catalyst, which excludes the possibility of C-H activation enhanced for 5S-2Pt/ZSM-5 catalyst during propane oxidation. Therefore, the increased catalytic activity of S-Pt/ZSM-5 can be ascribed to the activation of C-C bond in the propane. In order to differentiate the contribution of Pt and sulfate on propane oxidation, the comparison experiments of propane oxidation were carried out on 5 S/ZSM-5, 0.5Pt/ZSM-5, 0.5Pt/ZSM-5 + 5 S/ZSM-5 and 0.5Pt/ZSM-5 + 100 S/ZSM-5 (+, represents physical mixing) in Fig. 8b. The 0.5Pt/ZSM-5 with low activity was selected to significantly observe change in activity. It can be found the single 5 S/ZSM-5 catalyst is nearly inactive for propane oxidation, whereas the 5 S/ZSM-5 physically mixed into 0.5Pt/ZSM-5 catalyst can obviously enhance the activity of 0.5Pt/ZSM-5 catalyst, in particularly, the physical mixed 0.5Pt/ZSM-5 + 100 S/ZSM-5 shows much higher catalytic activity compared to the 0.5Pt/ZSM-5 catalyst. Combined with result previously discussed, the introduction of sulfate results in the promotion of C-C bond activation. The possible pathway of propane oxidation on 5S-2Pt/ZSM-5 is proposed in Fig. 8c. It is inferred that propane molecule firstly absorbs on the sulfate and is activated to intermediates by breaking C-C bond, then such intermediates transfers from sulfate to Pt species for deep oxidation. Gaseous oxygen adsorbed on Pt surface becomes active oxygen species and reacts with the intermediates to CO_2 and H_2O. This new synergistically catalysis reaction pathway, relative to the traditional C-H activation pathway, remarkably decreases the Ea (55.8 ± 6.0 kJ·mol^{-1}) of 5S-2Pt/ZSM-5, compared to 95.0 ± 7.3 kJ·mol^{-1} of 2Pt/ZSM-5, thus remarkably improving the catalyst activity.

Fig. 9 shows the Pt 4*d* XPS spectra, due to the overlapping of the Pt 4 *f* signal with Al 2*p*, of the parent 2Pt/ZSM-5 and sulfate modified 1Pt/ZSM-5, 2Pt/ZSM-5 and 3Pt/ZSM-5 catalysts. For the parent 2Pt/ZSM-5 catalyst, the components with binding energy at 314.6 and 316.7 eV are assigned to the Pt $4d_{5/2}$ spectra of surface Pt^0 and Pt^{2+} species, respectively [31,47,54]. It can be seen that Pt 4*d* spectra of sulfate modified Pt/ZSM-5 with lower Pt/S atomic ratio gradually shifts to higher binding energy compared to 2Pt/ZSM-5 catalyst, indicating Pt species electron deficiency. The electron deficient Pt species may be responsible for the decreased CO chemical uptake of sulfate modified Pt/ZSM-5 (Table 4). Burch *et al.* pointed out that Pt species interacts closely with sulfate and described there $Pt^{\delta+}$-$(SO_4^{2-})^{\delta-}$ couple in sulfate modified Pt/Al_2O_3 catalyst [55]. Therefore, it is inferred that there electron transfer from Pt species to sulfate takes place in the sulfate modified Pt/ZSM-5, as evidenced by decreased S 2*p* binding energy (Fig. 9c). In additionally, the proportion of Pt^0 specie in sulfate modified Pt/ZSM-5 catalyst decreases when Pt/S atomic ratio decreases. This result can be ascribed to that the increased strength of Pt and sulfate interaction caused by decreasing Pt/S atomic ratio, leading to oxidized Pt specie difficultly to be reduced. It is consistent with the result of H_2-TPR experiment as discussed in Fig. 4c. For Pt catalyst without sulfate modification, it is commonly recognized that Pt^0 specie is the crucial active sites for C-H activation in light alkane and oxidized Pt specie (PtO_x) enables the subsequent oxidation of intermediate products undergo [41]. Yet, it is worth noting that the parent 2Pt/ZSM-5 catalyst with higher Pt^0 ratio shows inferior catalytic activity compared to 5S-2Pt/ZSM-5 catalyst, such result is ascribed to that C-C activation mechanism driven by Pt and sulfate synergy catalysis plays critical role on propane activation in 5S-2Pt/ZSM-5 catalyst (Fig. 8c). Of course, increasing proportion of Pt^0 specie in 5S-2Pt/ZSM-5 catalyst would also enhance the catalytic activity for propane oxidation due to C-H activation ability increase, which will be discussed in Fig. 10 in following. Moreover, the synergy of Pt and sulfate is remarkably depended by their interaction strength (Fig. 5e), significantly affected by the Pt/S atomic ratio. The 2Pt/ZSM-5 catalyst has the moderate interaction strength of Pt and sulfate, thus exhibiting the optimizing catalytic activity for propane oxidation.

3.5. Stability of sulfate modified Pt/ZSM-5 catalyst

To investigate the thermal stability of the Pt/ZSM-5 catalysts, the catalytic activities of two 2Pt/ZSM-5 and 5S-2Pt/ZSM-5 catalysts for propane oxidation were evaluated at 220 °C for long time as shown in Fig. 10. Noticeably, these two catalysts all exhibit a induction period in the initial stage. For instance, propane conversion of the 2Pt/ZSM-5 catalyst increases from 48% to 64% within the first 3 hours, and

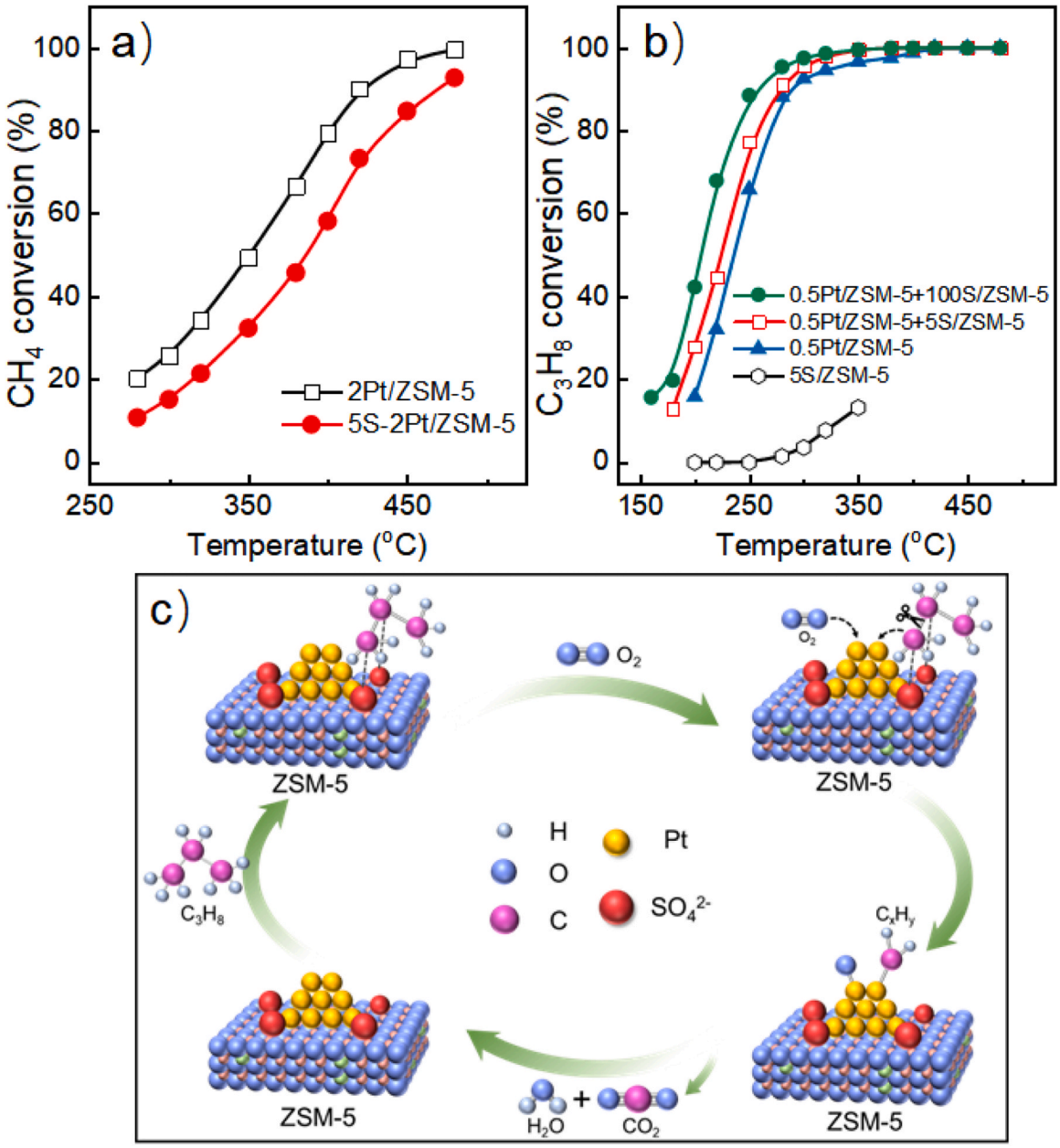

Fig. 8. a) methane oxidation activities of 5S2Pt/ZSM-5 and 2Pt/ZSM-5 catalysts, b) propane oxidation activities of 5 S/ZSM-5, 0.5Pt/ZSM-5, 0.5Pt/ZSM-5 + 5 S/ZSM-5 and 0.5Pt/ZSM-5 + 100 S/ZSM-5 (+, represents physical mixing), c) the possible reaction mechanism for sulfate and Pt species synergetic catalysis for propane oxidation.

propane conversion of the 5S-2Pt/ZSM-5 catalyst increases 64–71%. Previous works also observed the induction period of propane oxidation and ascribed such result to the generation of metallic Pt species, which promotes the propane activation on the catalyst surface through C-H activation mechanism [36,41]. Thus, the XPS characterization of spent catalyst was conducted to investigate the change of surface Pt species during propane oxidation (Fig. 9b). It can be found that the spent 5S-2Pt/ZSM-5 catalyst indeed has more surface Pt^0 specie compared to the fresh 5S-2Pt/ZSM-5 catalyst, the generated surface Pt^0 specie accounts for the induction period of propane oxidation. At this point, both the C-H activation mechanism and the C-C bond activation mechanism occur to catalyze propane oxidation simultaneously. The stable activity of 5S-2Pt/ZSM-5 catalyst after induction period confirms the robust structure of Pt species and sulfate modified in the catalyst.

Water steam in the feed gas often leads to the serious deactivation of Pt catalyst caused by water molecule competitive absorption on active sties [43]. Thus, much attention has also been paid to improve the water tolerance of catalyst. The propane oxidation reaction was conducted under staged reaction condition (0.2% C_3H_8 + 2% O_2 /N_2 balanced; 0.2% C_3H_8 + 2% O_2 + 5% H_2O/N_2 balanced) to study the influence of water steam (5% H_2O) on the catalytic activity (Fig. 10b-c). It can be found that the 2Pt/ZSM-5 catalyst suffers a serious deactivation when reaction condition switched from dry to wet. Whereas, it is interesting to find that the existence of water steam in feed gas only slightly affect the catalytic activity. The stable activity of the 5S-2Pt/ZSM-5 catalyst should be ascribed to the strong interaction between Pt species and sulfate species, which prevents the water molecule absorption on the active sites [56]. Therefore, introduction of sulfate species into Pt/ZSM-5 not only increase the catalytic activity but also improve the water tolerance.

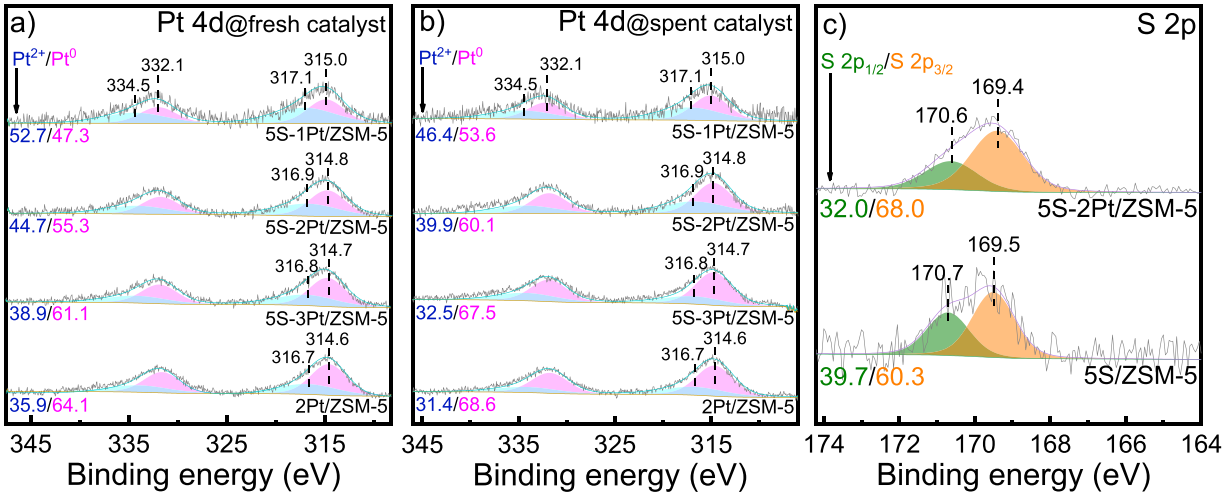

Fig. 9. XPS spectra Pt 4*d* of a) fresh and b) spent 2Pt/ZSM-5, 5S–1Pt/ZSM-5, 5S–2Pt/ZSM-5 and 5S–3Pt/ZSM-5 catalysts, c) S *2p*.

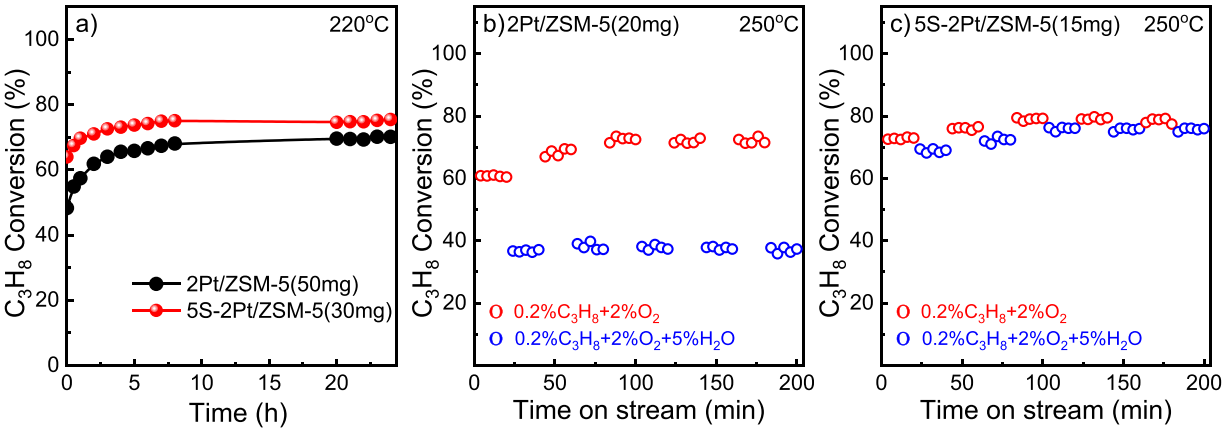

Fig. 10. a) The stability of propane oxidation over the Pt/ZSM-5 catalysts at 220 °C, b) and c) The stability of propane oxidation over the Pt/ZSM-5 catalysts under staged reaction condition at 250 °C.

4. Conclusion

In summary, we developed a novel sulfate modification in atomic level to promote supported Pt catalysts (Pt/ZSM-5, Pt/Al_2O_3, Pt/ZrO_2, Pt/CeO_2) for propane complete oxidation by in situ pyrolysis of $(NH_4)_2SO_4$ mixed with catalysts. Sulfate specie significantly enhances these catalysts performance for propane complete oxidation, particularly for ZSM-5 supported Pt catalyst. On one hand, Pt specie promotes the increase of sulfate when sulfate is low content. On the other hand, Pt species also boosts the sulfate decomposition when the S content is excessive or the Pt content is high. Therefore, the Pt/S atomic ratio in sulfate modified Pt/ZSM-5 catalyst can be adjusted by changing the amount of $(NH_4)_2SO_4$ used and Pt loading. It is found that the Pt/S atomic ratio remarkably affects the electron transfer from Pt species to sulfate and their interaction strength, which is closely related to their synergetic catalysis for propane activation. The 5S-2Pt/ZSM-5 with Pt/S atomic ratio of 0.5 presents moderate strength of sulfate and Pt species interaction, thus exhibiting the highest reaction rate. Our primary work provides the novel strategy to develop potential active industrial catalysts for light alkane catalytic elimination.

CRediT authorship contribution statement

Jian Chen: Writing – review & editing, Writing – original draft, Supervision, Methodology, Investigation, Conceptualization. **Wen-Xia Zhang:** Visualization, Validation, Software, Investigation. **Xiao-Hui Luo:** Validation, Resources, Investigation. **Cai-Hao Wen:** Visualization, Investigation, Formal analysis, Data curation. **Lin-Ya Xu:** Writing – original draft, Visualization, Software, Investigation, Data curation. **Meng-Fei Luo:** Writing – review & editing, Supervision, Project administration, Funding acquisition, Conceptualization. **Ji-Qing Lu:** Supervision, Project administration, Funding acquisition, Conceptualization. **Qi-Hua Yang:** Writing – review & editing, Supervision, Project administration, Methodology, Conceptualization. **Xi Zhao:** Validation, Software, Investigation, Data curation.

Declaration of Competing Interest

The authors declare that they have no known competing financial interests or personal relationships that could have appeared to influence the work reported in this paper.

Data availability

Data will be made available on request.

Acknowledgements

This work was financially supported by the National Natural Science Foundation of China (No. 22172145, 22072137) and the Leading Innovative and Entrepreneur Team Introduction Program of Zhejiang (No. 2022R01007).

Appendix A. Supporting information

Supplementary data associated with this article can be found in the online version at doi:10.1016/j.apcatb.2024.124135.

References

[1] Z. Li, R. Gao, Z. Hou, X. Yu, H. Dai, J. Deng, Y. Liu, Tandem supported Pt and ZSM-5 catalyst with separated catalytic functions for promoting multicomponent VOCs oxidation, Appl. Catal. B Environ. 339 (2023) 123–131.
[2] Y. Shen, J. Deng, X. Hu, X. Chen, H. Yang, D. Cheng, D. Zhang, Expediting toluene combustion by harmonizing the Ce-O strength over Co-doped CeZr oxide catalysts, Environ. Sci. Technol. 57 (2023) 1797–1806.
[3] Y. Ren, X. Lei, H. Wang, J. Xiao, Z. Qu, Enhanced catalytic performance of La-doped $CoMn_2O_4$ catalysts by regulating oxygen species activity for VOCs oxidation, ACS Catal. 13 (2023) 8293–8306.
[4] Y. Yang, W. Si, Y. Peng, J. Chen, Y. Wang, D. Chen, Z. Tian, J. Wang, J. Li, Oxygen vacancy engineering on copper-manganese spinel surface for enhancing toluene catalytic combustion: a comparative study of acid treatment and alkali treatment, Appl. Catal. B Environ. 340 (2024) 123–142.
[5] Y. Shen, J. Deng, S. Impeng, S. Li, T. Yan, J. Zhang, L. Shi, D. Zhang, Boosting toluene combustion by engineering Co-O strength in cobalt oxide catalysts, Environ. Sci. Technol. 54 (2020) 10342–10350.
[6] Z. Hou, M. Chen, Y. Liu, J. Deng, L. Jing, R. Gao, W. Pei, Z. Li, H. Dai, Enhanced moisture resistance and catalytic stability of ethylene oxidation at room temperature by the ultrasmall MnO_x cluster/Pt hetero-junction, Appl. Catal. B Environ. 339 (2023) 123115.
[7] Y. Ren, X. Lei, H. Wang, J. Xiao, Z. Qu, Enhanced catalytic performance of La-doped $CoMn_2O_4$ catalysts by regulating oxygen species activity for VOCs Oxidation, ACS Catal. 13 (12) (2023) 8293–8306.
[8] Y. Shen, J. Deng, L. Han, W. Ren, D. Zhang, Low-temperature combustion of toluene over Cu-doped $SmMn_2O_5$ mullite catalysts via creating highly active Cu^{2+}-O-Mn^{4+} sites, Environ. Sci. Technol. 56 (2022) 10433–10441.
[9] W. Zhu, X. Chen, C. Li, Z. Liu, C. Liang, Manipulating morphology and surface engineering of spinel cobalt oxides to attain high catalytic performance for propane oxidation, J. Catal. 396 (2021) 179–191.
[10] A. Yang, V. Streibel, T.S. Choksi, H. Aljama, B. Werghi, S. R. parent, R.S. Sánchez-Carrera, A. Schäfer, Y. Li, F. Abild-Pedersen, M. Cargnello, Insights and comparison of structure-property relationships in propane and propene catalytic combustion on Pd- and Pt-based catalysts, J. Catal. 401 (2021) 89–101.
[11] W. Tan, S. Xie, Y. Cai, H. Yu, K. Ye, M. Wang, W. Diao, L. Ma, S.N. Ehrlich, F. Gao, L. Dong, F. Liu, Surface lattice-embedded Pt single-atom catalyst on ceria-zirconia with superior catalytic performance for propane oxidation, Environ. Sci. Technol. 57 (33) (2023) 12501–12512.
[12] Q. Fu, S. Wang, T. Wang, D. Xing, X. Yue, M. Wang, S. Wang, Insights into the promotion mechanism of ceria-zirconia solid solution to ethane combustion over Pt-based catalysts, J. Catal. 405 (2022) 129–139.
[13] X. Tang, M. Wang, B. Tang, Y. Zhao, W. Zhan, Y. Guo, L. Wang, S. Dai, Y. Guo, Synthesis of heteroatom Pd-ZrO_x species on zeolite for complete methane oxidation, Ind. Eng. Chem. Res. 62 (21) (2023) 8244–8252.
[14] Z. Huang, J. Ding, X. Yang, H. Liu, P. Song, Y. Guo, Y. Guo, L. Wang, W. Zhan, Highly efficient oxidation of propane at low temperature over a Pt-Based catalyst by optimization support, Environ. Sci. Technol. 56 (23) (2022) 17278–17287.
[15] S. Wu, H. Liu, Z. Huang, H. Xu, W. Shen, O-vacancy-rich porous MnO_2 nanosheets as highly efficient catalysts for propane catalytic oxidation, Appl. Catal. B Environ. 312 (2022) 121387.
[16] Y. Ding, Y. Jia, M. Jiang, Y. Guo, Y. Guo, L. Wang, Q. Ke, M.N. Ha, S. Dai, W. Zhan, Superior catalytic activity of Pd-based catalysts upon tuning the structure of the ceria-zirconia support for methane combustion, Chem. Eng. J. 416 (2021) 129150.
[17] H. Gu, J. Lan, H. Hu, F. Jia, Z. Ai, L. Zhang, X. Liu, Surface oxygen vacancy-dependent molecular oxygen activation for propane combustion over α-MnO_2, J. Hazard. Mater. 406 (2023) 132499.
[18] J. Ji, C. Zhang, X. Yang, F. Kong, C. Wu, H. Duan, D. Yang, D. Yang, Pt-stabilized electron-rich Ir structures for low temperature methane combustion with enhanced sulfur-resistance, 2023, 466, 143044.
[19] Y. Gao, S. Wang, L. Lv, D. Li, X. Yue, S. Wang, Insights into the behaviors of the catalytic combustion of propane over spinel catalysts, Catal. Lett. 150 (2020) 3617–3625.
[20] J. Wu, B. Chen, J. Yan, X. Zheng, X. Wang, W. Deng, Q. Dai, Ultra-active Ru Supported on CeO_2 nanosheets for catalytic combustion of propane: Experimental insights into interfacial active sites, Chem. Eng. J. 438 (2022) 135501.
[21] B. Li, X. Zhao, X. Luo, W. Zhang, C. Wen, L. Xu, C. Tang, M. Luo, J. Chen, Boosting propane combustion over Pt/WO_3 catalyst by activating interface oxygen species, Appl. Surf. Sci. 650 (2024) 159225.
[22] Z. Huang, S. Cao, J. Yu, X. Tang, Y. Guo, Y. Guo, L. Wang, S. Dai, W. Zhan, Total Oxidation of light alkane over phosphate-modified Pt/CeO_2 catalysts, Environ. Sci. Technol. 56 (23) (2022) 17278–17287.
[23] Y. Ding, Q. Wu, B. Lin, Y. Guo, Y. Wang, L. Wang, W. Zhan, Superior catalytic activity of a Pd catalyst in methane combustion by fine-tuning the phase of ceria-zirconia support, Appl. Catal. B Environ. 266 (2022) 118631.
[24] R. Camposeco, O. Miguel, A.E. Torres, D.E. Armas, R. Zanella, Highly active Ru/TiO_2 nanostructures for total catalytic oxidation of propane, Environ. Sci. Pollut. Res. 30 (2023) 98076–98090.
[25] Y. Liu, H. Hu, J. Zheng, F. Xie, H. Gu, S. Rostamnia, F. Pan, X. Liu, L. Zhang, Interfacial engineering enables surface lattice oxygen activation of $SmMn_2O_5$ for catalytic propane combustion, Appl. Catal. B Environ. 330 (2023) 122649.
[26] X. Han, S. Jin, C. Rao, Y. Fang, B. Hu, K. Liu, Y. Zhang, X. Yang, Mo-modified Pt/CeO_2 nanorods with high propane catalytic combustion activity: Comparison of phosphoric, sulphuric and molybdic acid modifications, Mol. Catal. 548 (2023) 113426.
[27] H. Xia, Y. Bai, Q. Niu, B. Chen, F. Wang, B. Gao, L. Liu, X. Wang, W. Deng, Q. Dai, Support-dependent activity and thermal stability of Ru-based catalysts for catalytic combustion of light hydrocarbons, Ind. Eng. Chem. Res. 62 (4) (2023) 1826–1838.
[28] J. Wu, B. Chen, J. Yan, X. Zheng, X. Wang, W. Deng, Q. Dai, Ultra-active Ru supported on CeO_2 nanosheets for catalytic combustion of propane: experimental insights into interfacial active sites, Chem. Eng. J. 438 (2022) 135501.
[29] Y. Yazawa, N. Takagi, H. Yoshida, S. Komai, A. Satsuma, T. Tanaka, S. Yoshida, T. Hattori, The support effect on propane combustion over platinum catalyst: control of the oxidation-resistance of platinum by the acid strength of support materials, Appl. Catal. A Gen. 233 (2002) 103–112.
[30] Y. Yazawa, H. Yoshida, T. Hattori, The support effect on platinum catalyst under oxidizing atmosphere: improvement in the oxidation-resistance of platinum by the electrophilic property of support materials, Appl. Catal. A Gen. 237 (2002) 139–148.
[31] X. Wang, C. Liu, L. He, B. Li, J. Lu, M. Luo, J. Chen, Unveiling geometric and electronic effects of Pt species on water-tolerant Pt/ZSM-5 catalyst for propane oxidation, Appl. Catal. A Gen. 655 (2023) 119108.
[32] Z.Z. Zhu, G.Z. Lu, Y. Guo, Y.L. Guo, Z.G. Zhang, Y.Q. Wang, X.Q. Gong, High performance and stability of the Pt-W/ZSM-5 catalyst for the total oxidation of propane: the role of tungsten, ChemCatChem 5 (2013) 2495–2503.
[33] Y. Yazawa, H. Yoshid, S. Komai, T. Hattori, The additive effect on propane combustion over platinum catalyst: Control of the oxidation-resistance of platinum by the electronegativity of additives, Appl. Catal. A Gen. 233 (2002) 113–124.
[34] X. Wu, L. Zhang, D. Weng, S. Liu, Z. Si, J. Fan, Total oxidation of propane on Pt/WO_x/Al_2O_3 catalysts by formation of metastable Pt_i^+ species interacted with WO_x clusters, J. Hazard. Mater. 225-226 (2012) 146–154.
[35] W.M. Liao, Y.R. Liu, P.P. Zhao, B.H. Cen, C. Tang, A.P. Jia, J.Q. Lu, M.F. Luo, Total oxidation of propane over Pt-V/SiO_2 catalysts: remarkable enhancement of activity by vanadium promotion, Appl. Catal. A Gen. 590 (2020) 117337.
[36] P. Zhao, W. Wang, X. Wang, C. Liu, J. Lu, M. Luo, J. Chen, The effects of MoO_3 impregnation order on the catalytic activity for propane combustion over Pt/ZrO_2 catalysts: The crucial roles of Pt-MoO_3 interfacial sites density, N. J. Chem. 45 (2021) 14695–14702.
[37] W. Liao, X. Fang, B. Cen, J. Chen, Y. Liu, M. Luo, J. Lu, Deep oxidation of propane over WO_3-promoted Pt/BN catalysts: the critical role of Pt-WO_3 interface, Appl. Catal. B Environ. 272 (2020) 118858.
[38] S. Wang, S. Wang, X. Zong, S. Wang, X. Dong, CO oxidation with Pt catalysts supported on different supports: a comparison of their sulfur tolerance properties, Appl. Catal. A Gen. 654 (2023) 119083.
[39] H. Hao, B. Jin, W. Liu, X. Wu, F. Yin, S. Liu, Robust Pt@TiO_x/TiO_2 catalysts for hydrocarbon combustion: effects of Pt-TiO_x interaction and sulfates, ACS Catal. 10 (2020) 13543–13548.
[40] A.F. Lee, K. Wilson, R.M. Lambert, C.P. Hubbard, R.G. Hurley, R.W. McCabe, H. S. Gandhi, The origin of SO_2 promotion of propane oxidation over Pt/Al_2O_3 catalysts, J. Catal. 184 (1999) 491–498.
[41] X. Li, Y. Liu, W. Liao, A. Jia, Y. Wang, J. Lu, M. Luo, Synergistic roles of Pt^0 and Pt^{2+} species in propane combustion over high-performance Pt/AlF_3 catalysts, Appl. Surf. Sci. 475 (2019) 524–531.
[42] J.M. Grau, V.M. Benitez, J.C. Yori, C.R. Vera, J.F. Padilha, L.A. Magalhaes Pontes, A.O.S. Silva, Isomerization cracking of n-octane and n-decane on regulated acidity Pt/WO_x-SO_4-ZrO_2 catalysts, Energy Fuels 21 (3) (2007) 1390–1395.
[43] D. Li, X. Leng, X. Wang, H. Yu, W. Zhang, J. Chen, J. Lu, M. Luo, Unraveling the promoting roles of sulfate groups on propane combustion over Pt-SO_4^{2-}/ZrO_2 catalysts, J. Catal. 407 (2022) 322–332.
[44] C. Hu, C. Fang, Y. Lu, Y. Wang, J. Chen, M. Luo, Selective oxidation of diethylamine on CuO/ZSM-5 catalysts: the role of cooperative catalysis of CuO and surface acid sites, Ind. Eng. Chem. Res. 59 (20) (2020) 9432–9439.
[45] Y. Lu, C. Hu, W. Zhang, Z. Jin, X. Leng, Y. Wang, J. Chen, M. Luo, Promoting the selective catalytic oxidation of diethylamine over MnO_x/ZSM-5 by surface acid centers, Appl. Surf. Sci. 521 (2020) 146348.
[46] P. Zhao, J. Chen, H. Yu, B. Cen, W. Wang, M. Luo, J. Lu, Insights into propane combustion over MoO_3 promoted Pt/ZrO_2 catalysts: the generation of Pt-MoO_3 interface and its promotional role on catalytic activity, J. Catal. 391 (2020) 80–90.

[47] P. Zhao, X. Li, W. Liao, Y. Wang, J. Chen, J. Lu, M. Luo, Understanding the role of NbO_x on Pt/Al_2O_3 for effective catalytic propane oxidation, Ind. Eng. Chem. Res. 58 (48) (2019) 21945–21952.
[48] W. Wang, D. Li, H. Yu, C. Liu, C. Tang, J. Chen, J. Lu, M. Luo, Insights into different reaction behaviors of propane and CO oxidation over Pt/CeO_2 and Pt/Nb_2O_5: the crucial roles of support properties, J. Phys. Chem. C. 125 (35) (2021) 19301–19310.
[49] S. Song, Q. Liu, J. Xiong, M. Wen, T. An, Promotional effects of Ag on catalytic combustion of cyclohexane over PdAg/Ti-SBA-15, J. Catal. 421 (2023) 77–87.
[50] L. He, H. Xu, X. Leng, L. Jin, A. Jia, M. Luo, J. Chen, Boosting diethylamine selective oxidation over CuO/ZSM-5 catalyst by CeO_2 modification, Fuel 342 (2023) 127792.
[51] K. Wilson, C. Hardacre, R.M. Lambert, SO_2-promoted chemisorption and oxidation of propane over Pt (111), J. Phys. Chem. 99 (38) (1995) 13755–13758.
[52] A. Hinz, M. Skoglundh, E. Fridell, A. Andersson, An investigation of the reaction mechanism for the promotion of propane oxidation over Pt/Al_2O_3 by SO_2, J. Catal. 201 (2001) 247–257.
[53] C.P.O. Brien, I.C. Lee, A detailed spectroscopic analysis of the growth of oxycarbon species on the surface of Pt/Al_2O_3 during propane oxidation, J. Catal. 347 (2017) 1–8.
[54] G. Corro, J.L.G. Fierro, V.C. Odilon, , An XPS evidence of Pt^{4+} present on sulfated Pt/Al_2O_3 and its effect on propane combustion, Catal. Comm. 4 (2003) 371–376.
[55] R. Burch, E. Halpin, M. Hayes, K. Ruth, J.A. Sullivan, The nature of activity enhancement for propane oxidation over supported Pt catalysts exposed to sulphur dioxide, Appl. Catal. B Environ. 19 (1998) 199–207.
[56] X. Wang, L. Xu, C. Wen, D. Li, B. Li, J. Lu, Q. Yang, M. Luo, J. Chen, WO_3 boosted water tolerance of Pt nanoparticle on SO_4^{2-}-ZrO_2 for propane oxidation, Appl. Catal. B Environ. 338 (2023) 123000.